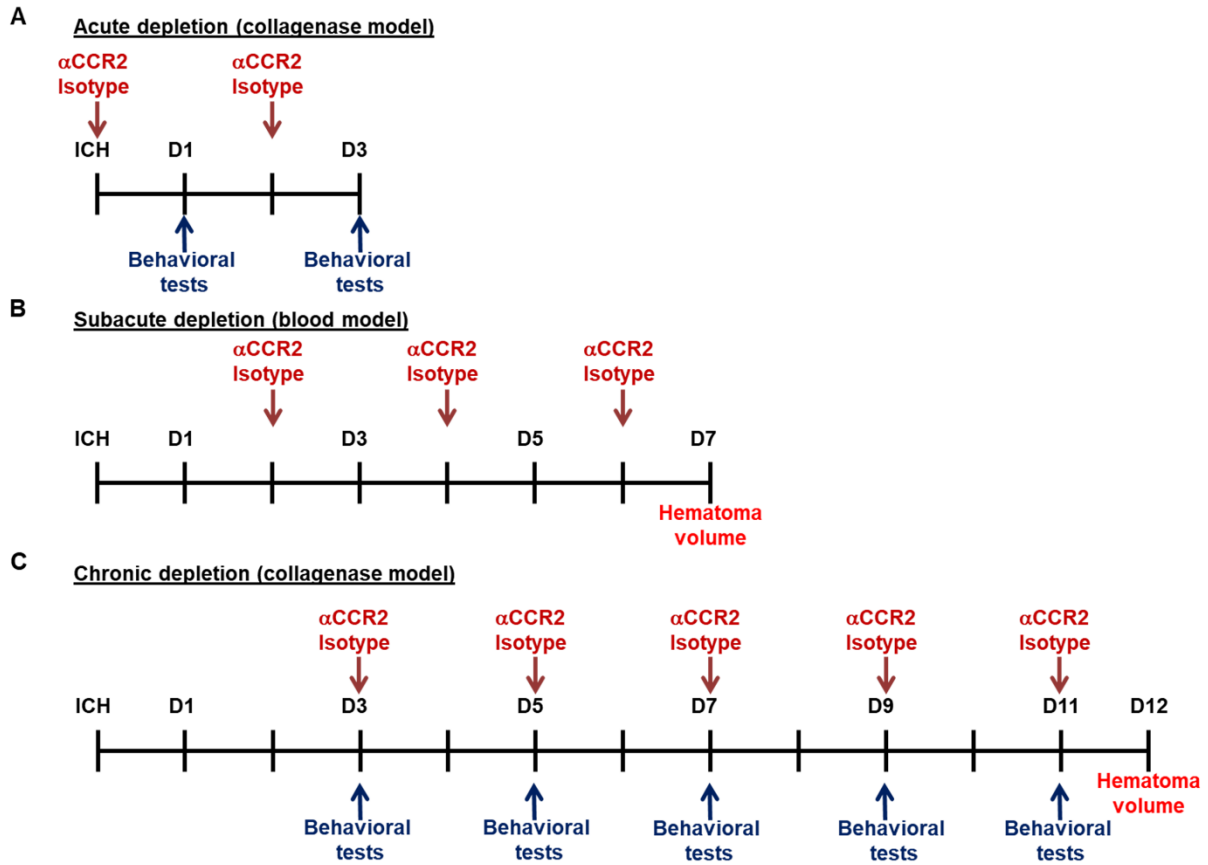
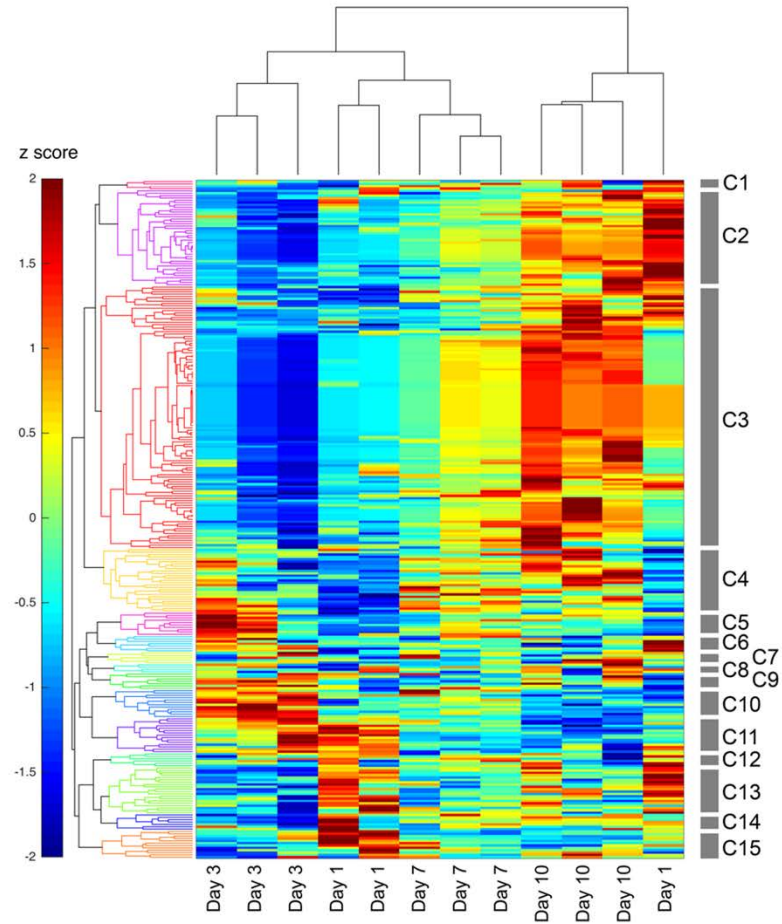


Supplemental Figure 1. Hematoma clearance in blood model of ICH. Top, representative brain coronal sections show brain hematoma from days 1, 3, and 7 ICH WT after blood injection model surgery. Bottom, Scatter plot of hematoma volume shows 29% and 68% reduction of hematoma volume from days 1 to 3 and from days 3 to 7, respectively. $n = 8$ for day 1; $n = 3$ for day 3; $n = 3$ for day 7. Data represent individual mice. * $P < 0.05$ versus day 1 or day 3 group by Student's t-test.



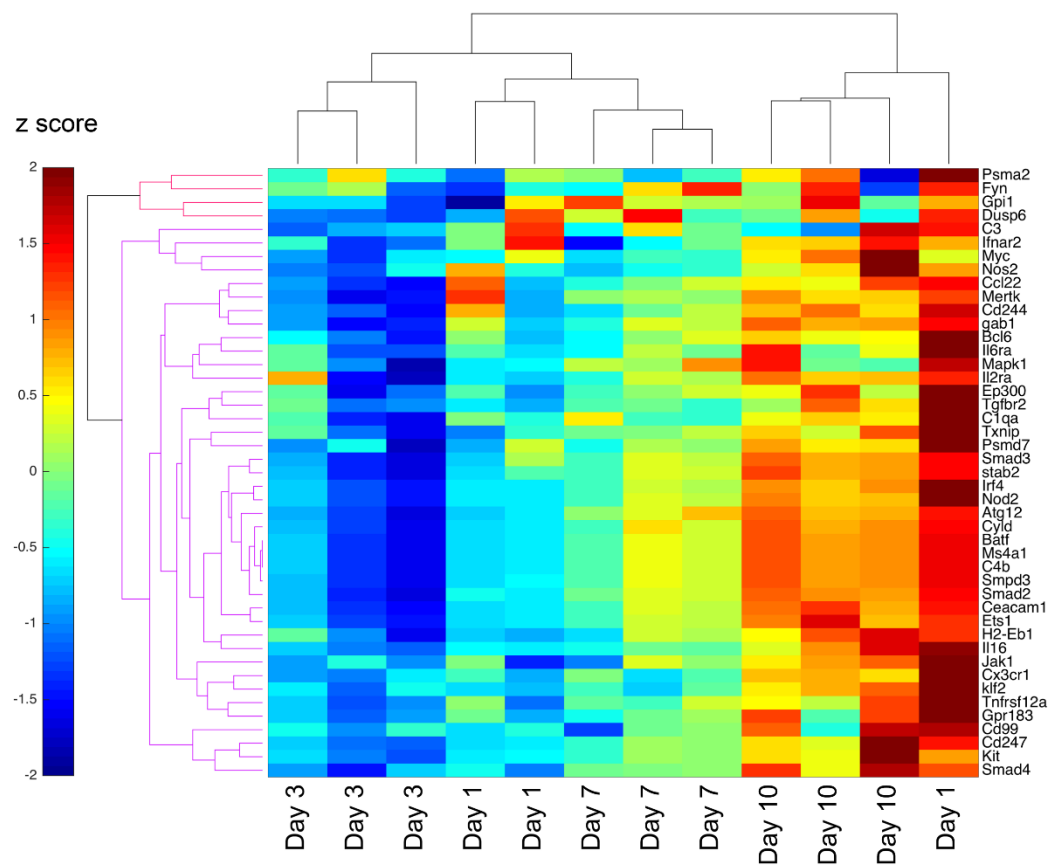
Supplemental Figure 2. Experimental design of peripheral monocyte depletion in preclinical models of ICH. (A) Acute depletion days 0-3, collagenase model, (B) subacute depletion, blood model, for day 7 hematoma quantification, (C) chronic depletion, collagenase model, for long-term behavior and hematoma quantification.

A

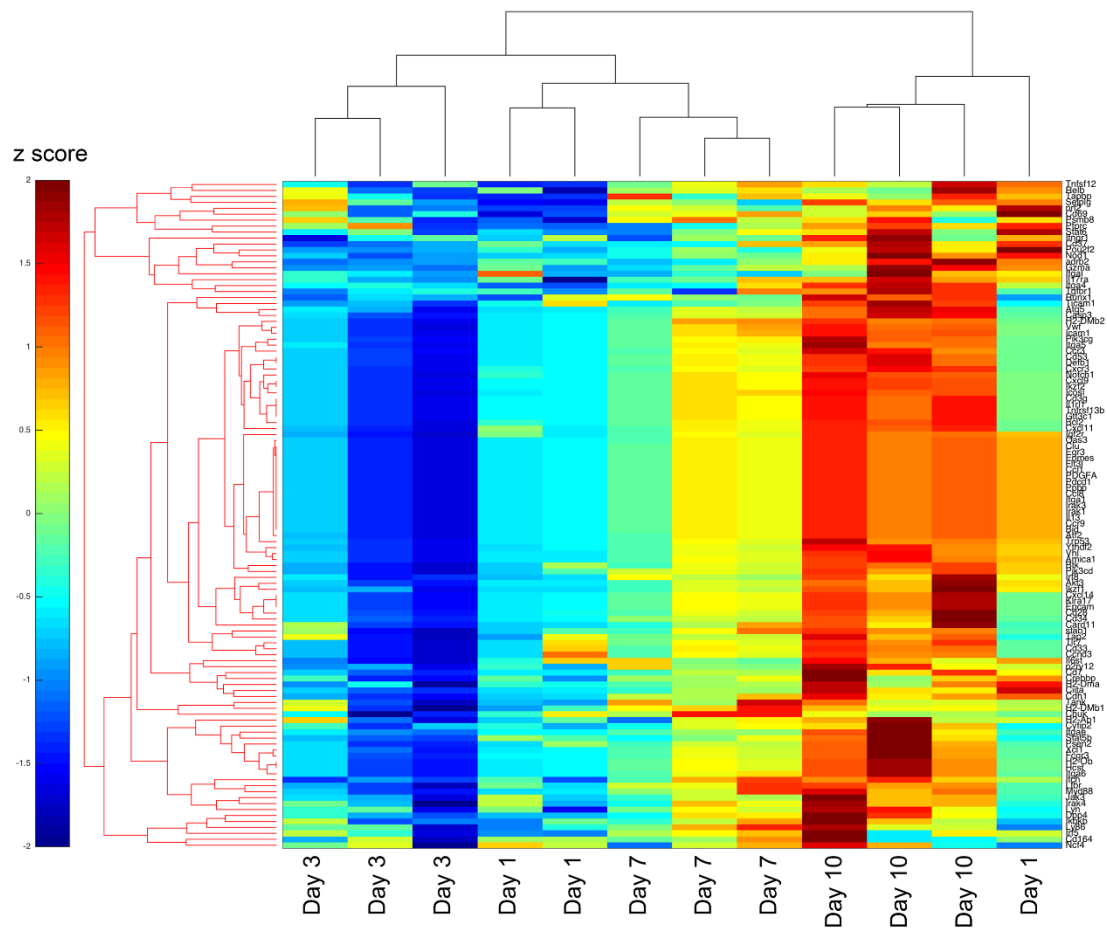


Supplemental Figure 3. Heat maps of all genes used for principal components analysis. The entire filtered gene set is shown (A) followed by enlargements of each cluster for clarity (B-F).

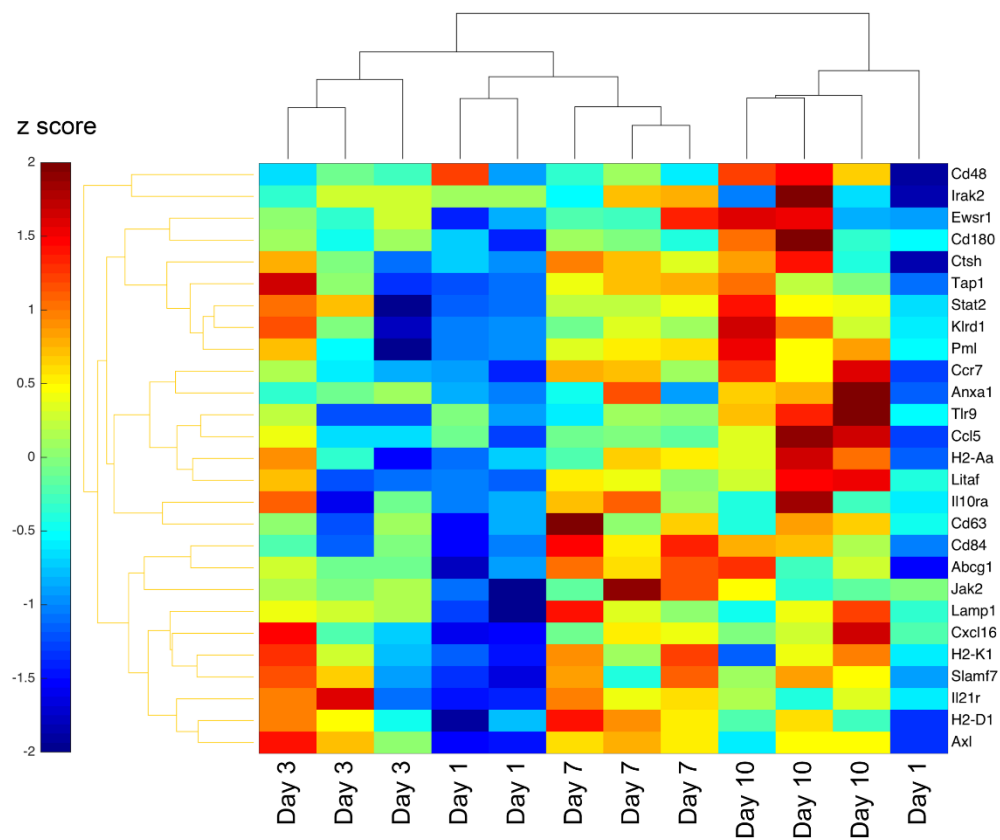
B



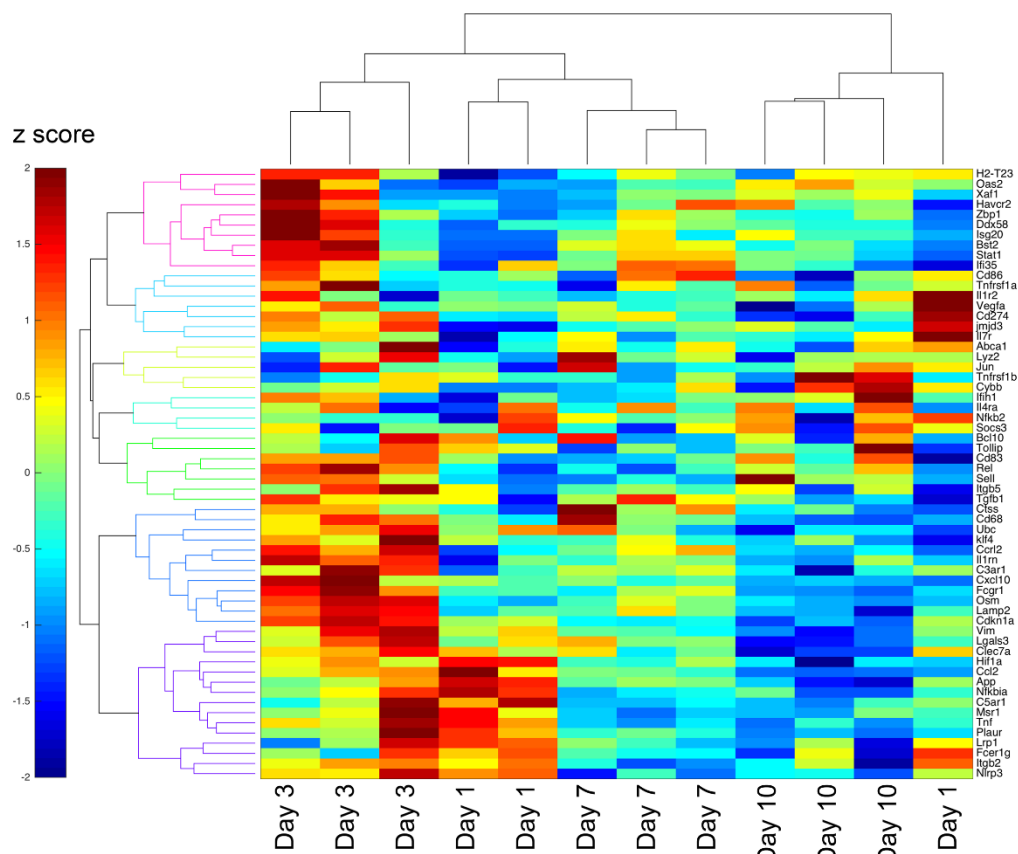
C



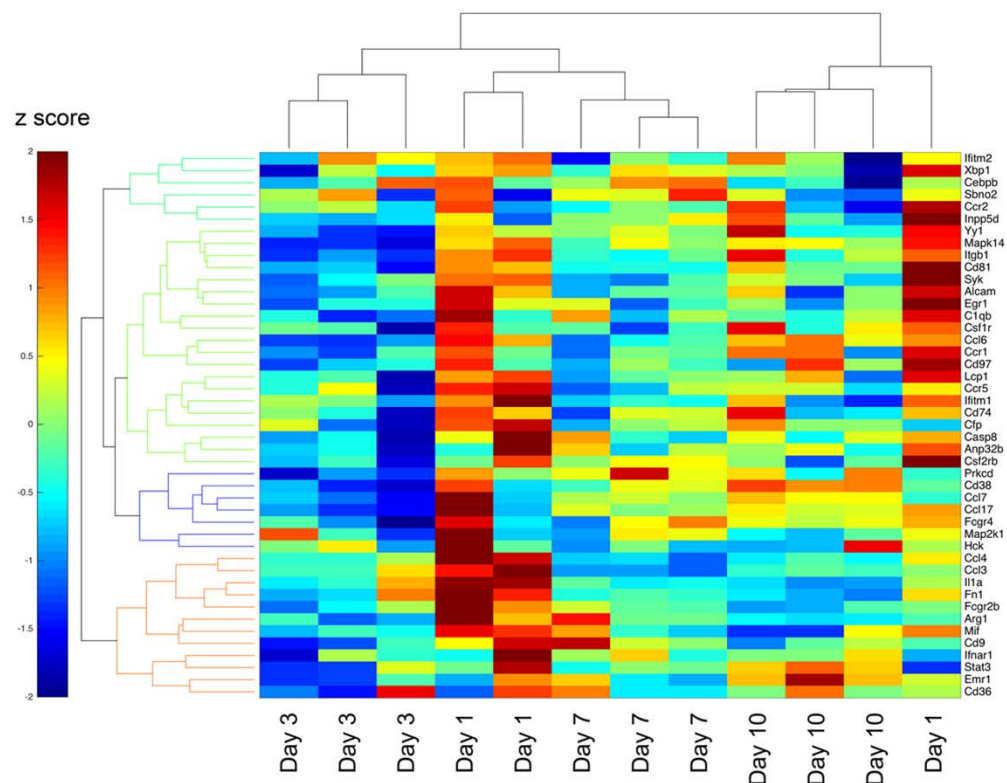
D

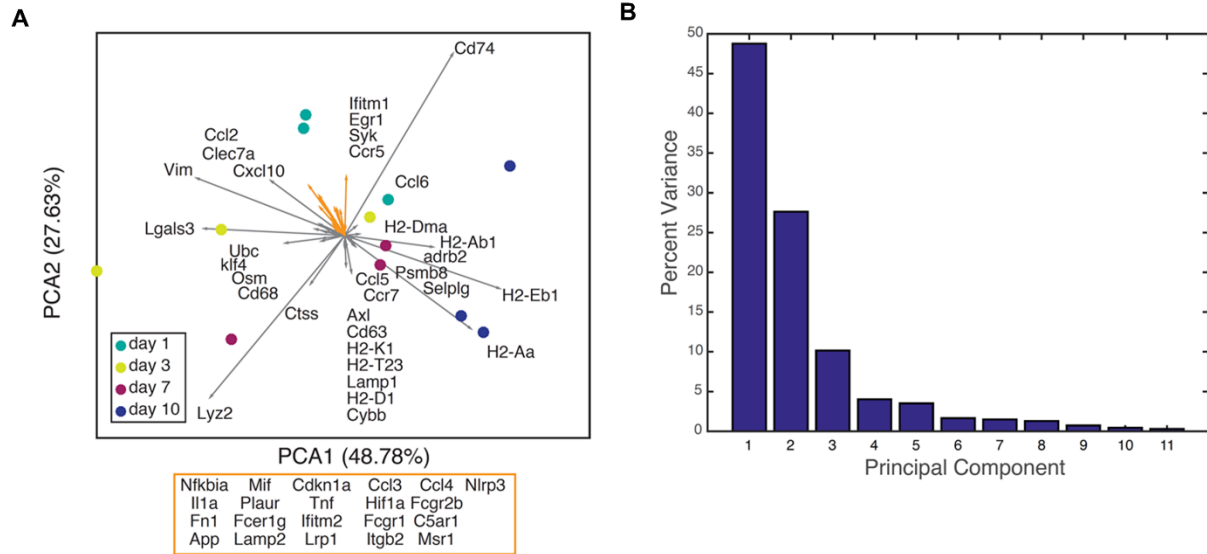


E

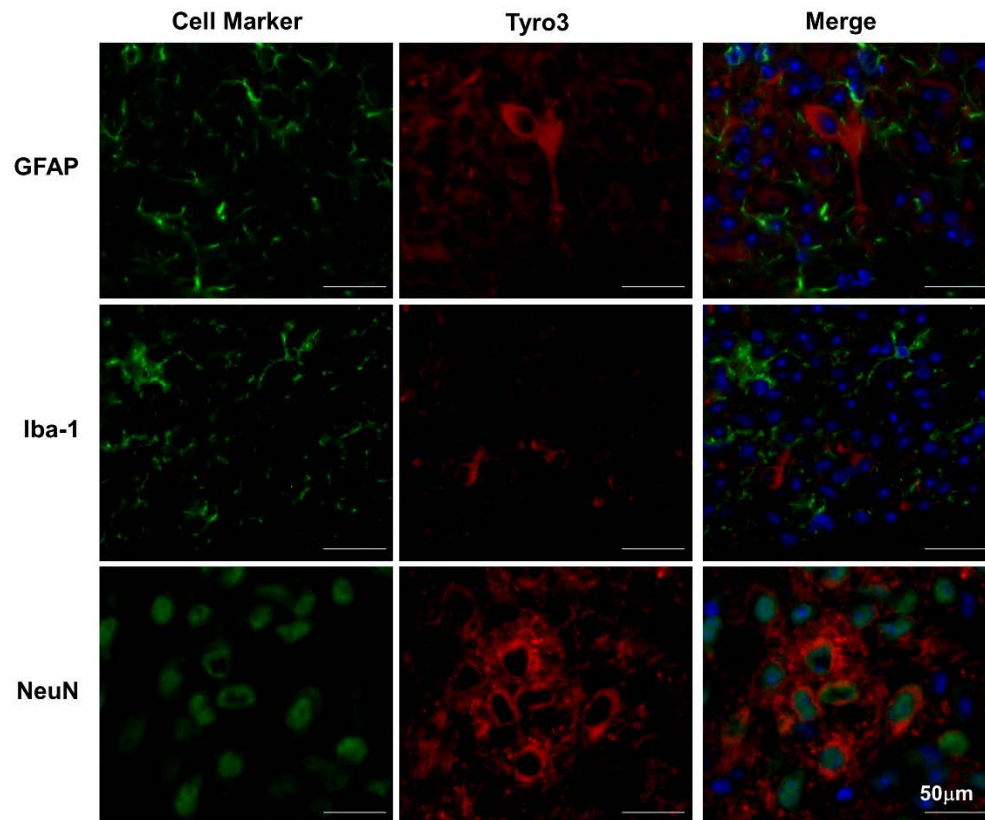


F

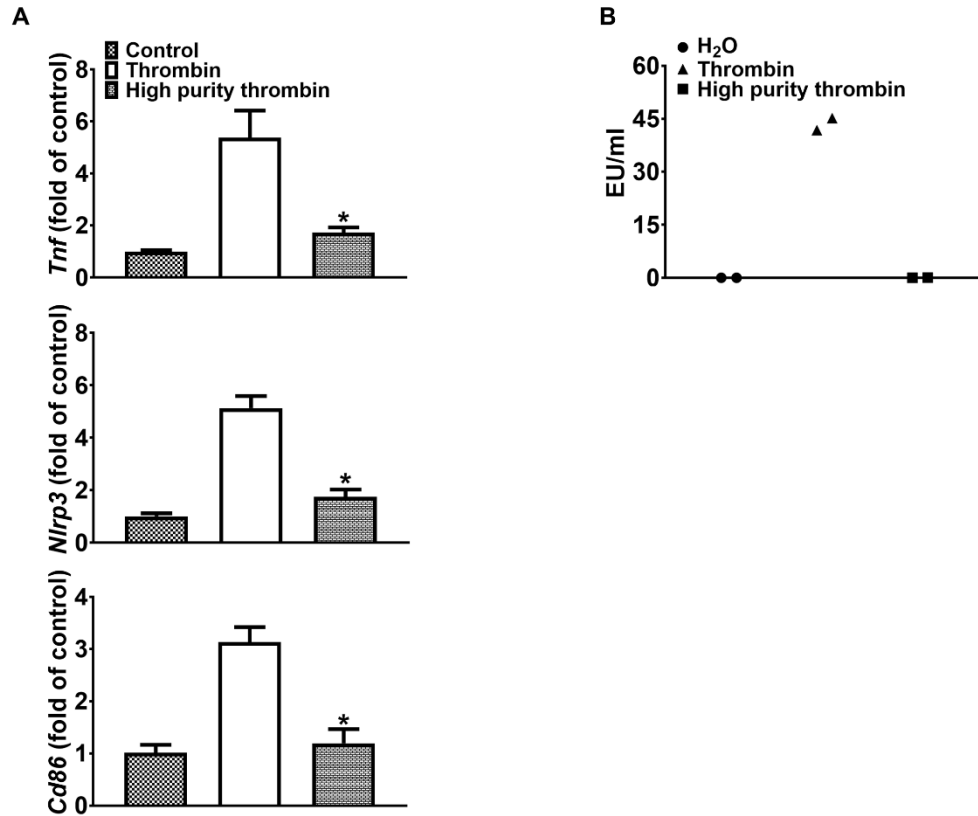




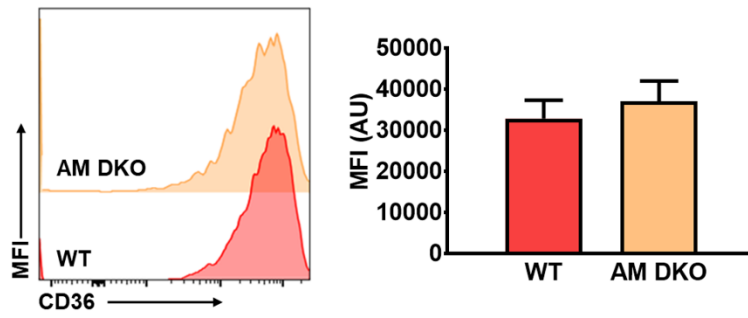
Supplemental Figure 4. Principal components analysis of MDMs transcriptome profile. (A) Scatter plot shows each sample projected on the first two principal components and are color coded according to time point. Genes are shown as projections along the first two components, and those that contribute significantly are labeled. Genes identified by the yellow projections are listed in the yellow box for legibility. **(B)** Percent variance explained by each principal component.



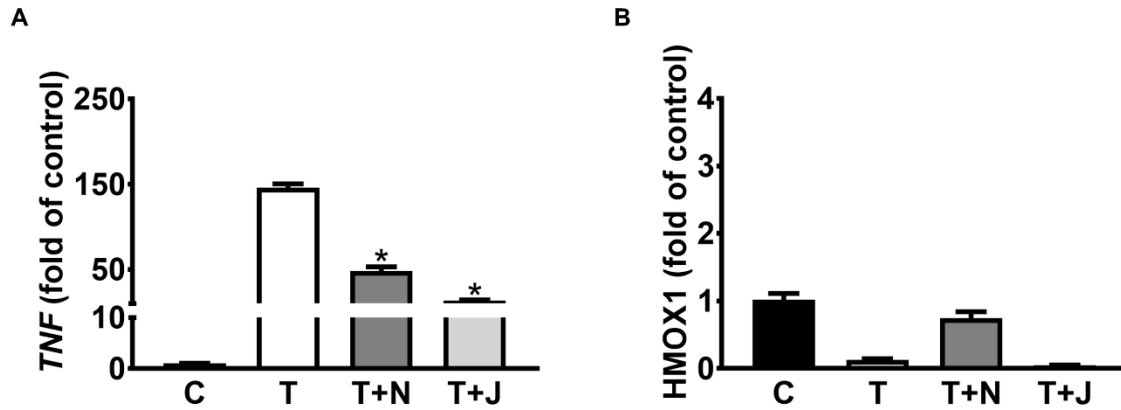
Supplemental Figure 5. Cellular localization of Tyro3 in the brain after ICH. Representative immunofluorescence images show Tyro3 immunoreactivity in red, and immunolabeling of GFAP (astrocytes), Iba1 (microglia/macrophages), or NeuN (neurons) in green in brain sections day 3 after ICH. Sections were stained with DAPI (blue) to show all nuclei.



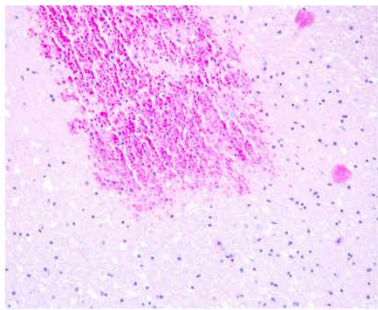
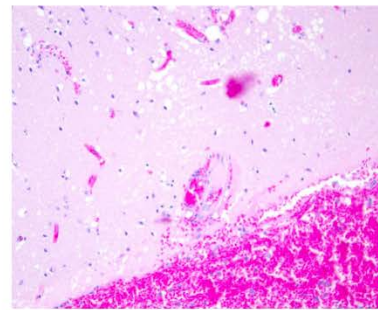
Supplemental Figure 6. Comparison of pro-inflammatory gene expression in BMDMs after thrombin and high purity thrombin stimulation. (A) Gene expression of *Tnf*, *Nlrp3*, and *Cd86* in BMDMs after different thrombin stimulations for 14h. Standard thrombin replicated the in vivo gene expression from MDMs from the brains on post-ICH day 1. n = 3 per group. * $P < 0.05$ versus control group by one-way ANOVA and Bonferroni's *post hoc* test. (B) Detection of LPS in the thrombin preparations were compared by limulus amebocyte lysate (LAL) assay (Associates of Cape Cod Inc) according to manufacturer's instructions. To eliminate enzymatic activity, thrombin preparations were incubated at 100 °C for 5 minutes prior to measurement. The kinetic measurement method with a threshold optical density value of 0.3 was used to calculate concentrations. Data represent individual experiments, each also included two technical duplicates. Thrombin preparations were obtained from Sigma (Standard: T6884, High purity: T1063).



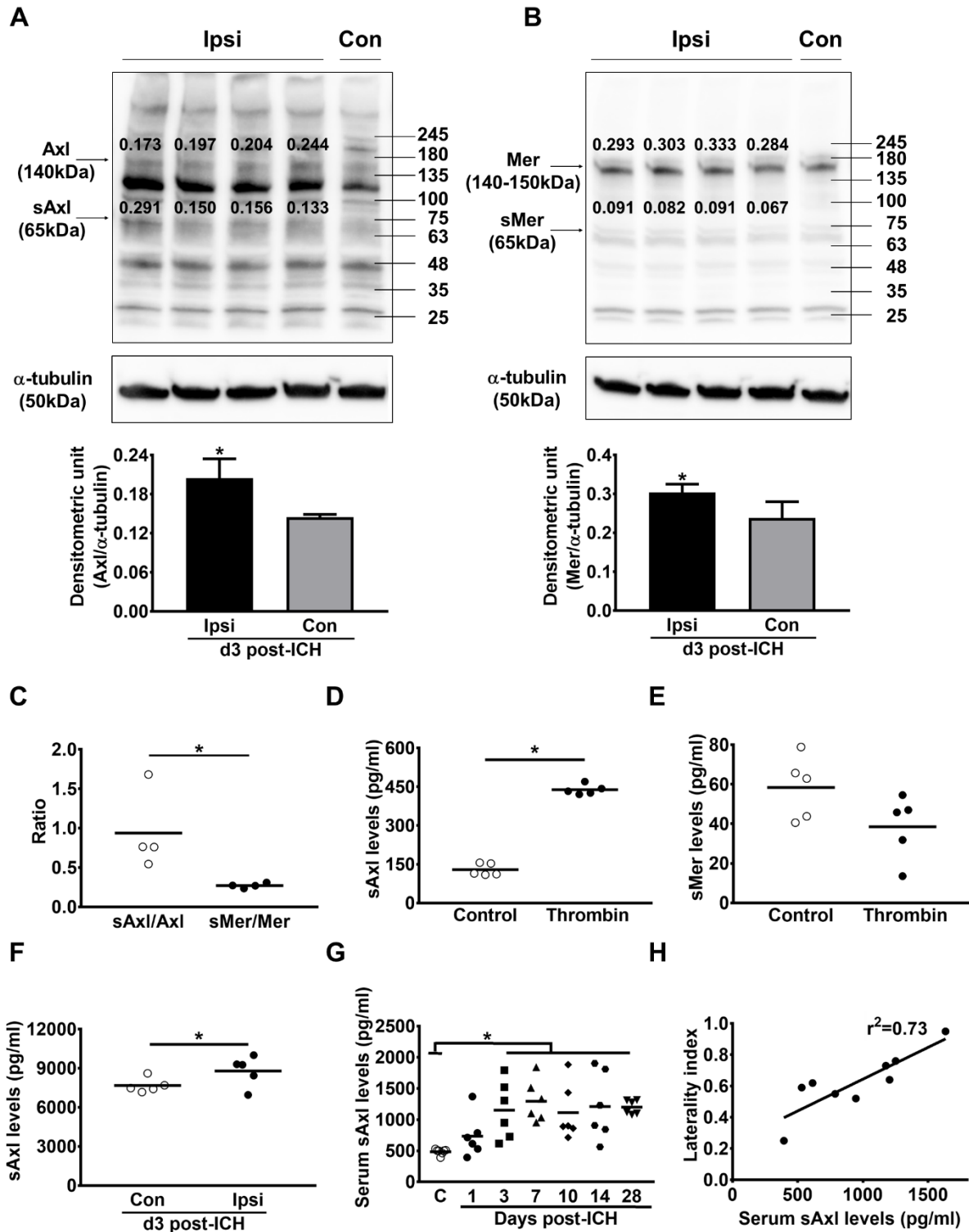
Supplemental Figure 7. *Axl* and *Mertk* deficiency does not affect baseline levels of CD36 expression on BMDM. Left, representative histogram shows CD36 expression on WT and AM DKO BMDM. Right, quantification of mean fluorescence intensity shows no difference in CD36 expression between WT and AM DKO BMDM. n = 6/group.



Supplemental Figure 8. Efferocytosis of neutrophils or Jurkat T cells reduces proinflammatory gene *TNF* expression, but does not induce *HMOX1* expression. Gene expression of *TNF* and *HMOX1* in human macrophages after thrombin, thrombin+N, thrombin+J stimulation for 6h. n = 3 different human donors/group; each independent experiment includes two technical replicates. * $P < 0.05$ versus thrombin group by one-way ANOVA and Bonferroni's *post hoc* test. C, control; T, thrombin; N, neutrophils; J, Jurkat T cells.

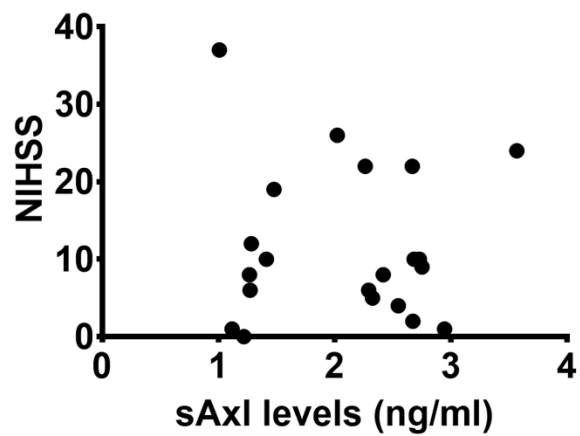
A**B**

Supplemental Figure 9. Representative noncontrast head CT scan images and H&E staining of perihematomal brain sections from the location indicated by rectangle for the patients in Fig. 6. (A) 39 year old female with history of sickle cell disease and Moya Moya syndrome who died almost immediately after ICH. **(B)** 34 year old male with history of arteriovenous malformation. Three days elapsed from ICH onset until death.



Supplemental Figure 10. Soluble Axl and Mer(tk) levels in serum and brain tissue after ICH induction and correlation between sAxl levels and functional deficit. Representative immunoblots of

the soluble and total **(A)** Axl and **(B)** Mer in the ipsilateral and contralateral brains of mice subjected to ICH surgery. Bar graph of densitometric analysis of bands showing significant increase in Axl and Mer protein level in the ipsilateral brains at 3 day post-ICH. The number above individual bands shows relative densitometric unit normalized to the corresponding α -tubulin (loading control) intensity in each sample. n = 4 for ipsilateral; n = 3 for contralateral. * $P < 0.05$ versus contralateral by Student's t -test. **(C)** Ratio of sAxl/Axl and sMertk/Mertk in the ipsilateral brains at day 3 post-ICH. n = 4/group. * $P < 0.05$ by Student's t -test. **(D)** sAxl and **(E)** sMer levels in control and 14h thrombin-stimulated BMDM culture medium by ELISA. n = 5/ group. * $P < 0.05$ by Student's t -test. Each dot represents an independent experiment, each included two technical replicates. **(F)** sAxl levels in the contralateral and ipsilateral brain tissues by ELISA at day 3 post-ICH. n = 5/group. * $P < 0.05$ versus contralateral by Student's t -test. **(G)** sAxl levels from control mice and mice on days 1, 3, 7, 10, 14, and 28 post-ICH. n = 6/group. * $P < 0.05$ versus control by one way ANOVA followed by Bonferroni's *post hoc* test. **(H)** Scatter plot show the correlation between serum sAxl levels and severity of laterality index by cylinder testing in each mouse at day 3 post-ICH. n = 9.



Supplemental Figure 11. No correlation between NIHSS and plasma sAXL levels in day 3 ICH patient samples. n = 21. NIHSS, NIH Stroke Scale.

Supplemental Table 1. Ordinal logistic regression of the association of circulating Mertk levels and functional outcome by modified Rankin Scale score at 1 year, adjusting for ICH score.

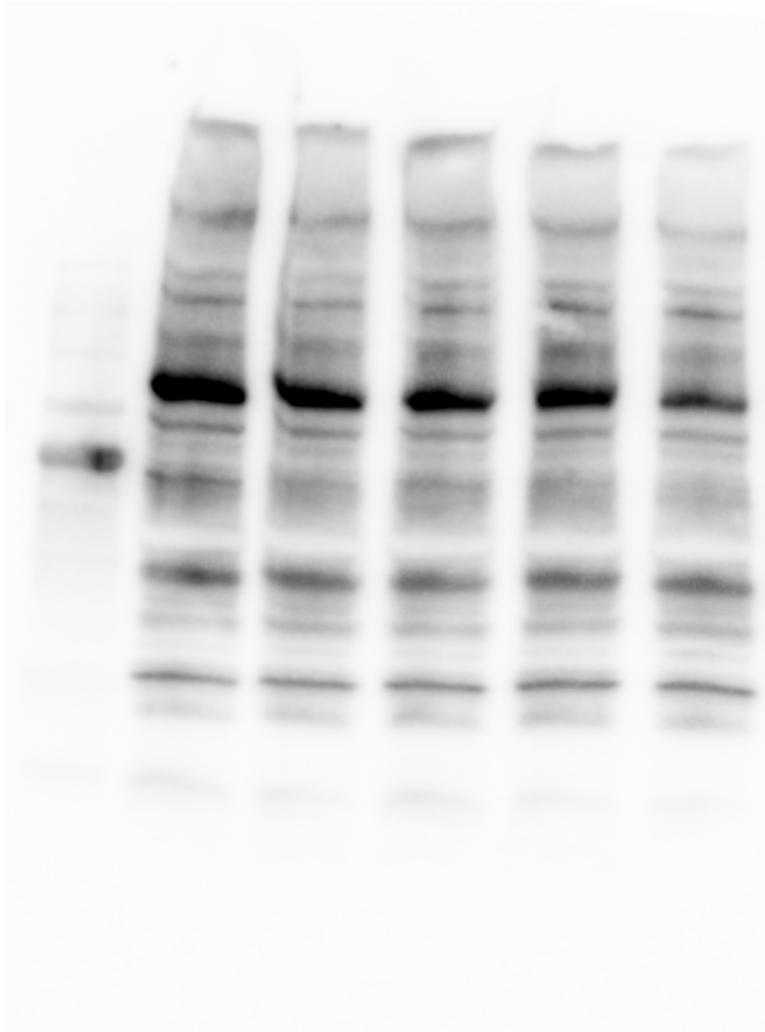
	OR	95% CI	p
ICH score	8.69	2.32-3.90	0.001
Mertk level at 72 hours	0.69	0.20-2.33	0.55

OR, Odds Ratio; CI, Confidence Interval. n=20.

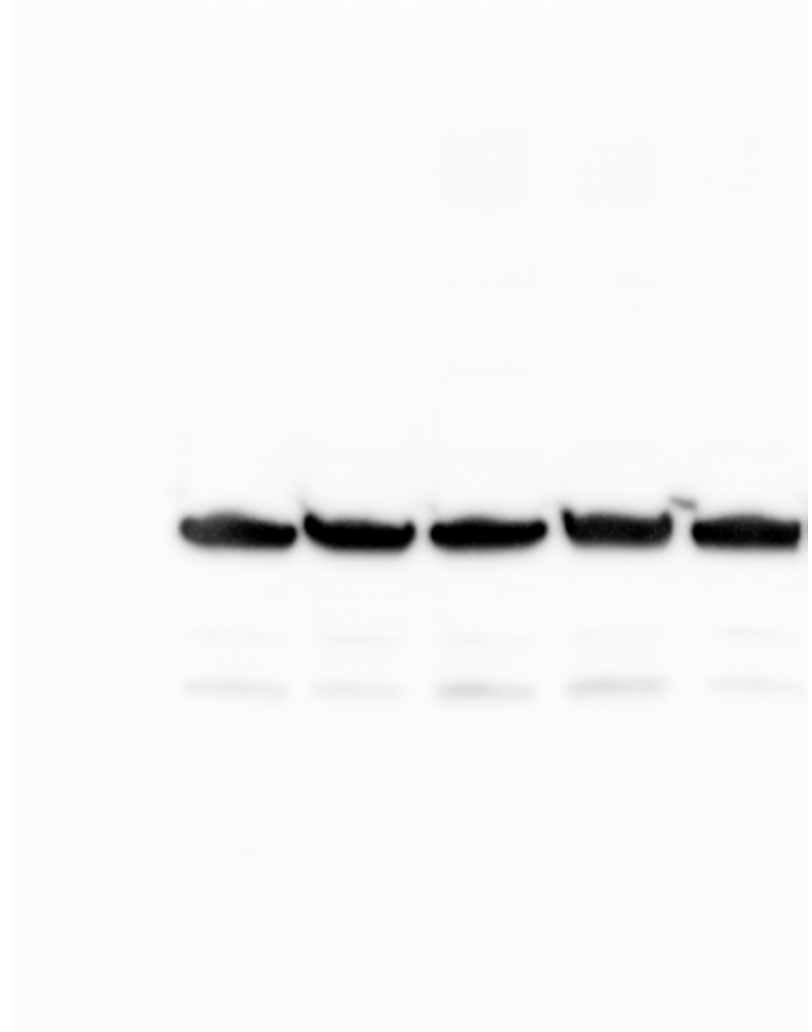
Unedited gel for Supplemental Figure 10A

Full gel is presented in the figure and each lane is corresponded to the representative plot

Axl



α -tubulin



Unedited gel for Supplemental Figure 10B

Full gel is presented in the figure and each lane is corresponded to the representative plot

Mer

α -tubulin

